Project 2 - Building Built in Minutes- SfM and NeRF

Using 1 late day

Karthik Mundanad
Robotics Engineering Department
Worcester Polytechnic Institute
Email: krmundanad@wpi.edu

Kushagra Srivastava
Robotics Engineering Department
Worcester Polytechnic Institute
Email: ksrivastava1@wpi.edu

***Abstract*—This report presents our implementation of a sparse 3D reconstruction framework for a given set of images using multi-view geometry. We present a detailed analysis of all the major steps involved in Structure from Motion qualitatively and quantitatively.**

I. Phase 1: Structure from Motion (SfM)

Our task was to construct a sparse 3D point cloud given a finite set of images. Our framework comprises 7 steps: (i) Estimation of the fundamental matrix using a given set of matched features, (ii) Estimation of the essential matrix, (iii) Camera pose estimation from the essential matrix, (iv) Linear and non-linear triangulation subjected to cheriality constraints, (v) Adding n^{th} image using perspective-n-point, (vi) Global optimization using bundle adjustment.

A. Estimation of the fundamental matrix using a given set of matched features

The first step in our framework is to estimate the fundamental matrix given a set of matched features based on the epipolar constraints using RANSAC. We found that using the 7-point algorithm instead of the 8-point algorithm is more robust since the probability of no outliers is exponential in the size of the sample set (see Section 11.6 in [1]).

Let $x_j \in R^{n\times3\times1}$ and $x_i \in R^{n\times1\times3}$ be matrices of homogenized matched feature image coordinates for i^{th} and j^{th} image respectively. Our goal is to find a solution for the fundamental matrix, $F \in R^{3\times3}$, such that Equation 1 is satisfied.

$$x_j^T F x_i = 0 \tag{1}$$

This equation gives rise to a set of equations of the form $Af = 0$, where $f \in R^{9\times1}$ is a vector of all entries in F and A is a function of the matched image coordinates for the image pair. It is possible to solve for f if the rank of A is 7 by making use of the singularity constraint. The solution of $Af = 0$, is in the form

$$\alpha F_1 + (1-\alpha)F_2 \tag{2}$$

where α is a scalar variable. The matrices F_1 and F_2 are obtained by solving for the right null space of A. Using the constraint $det(F) = 0$ which implies $det(\alpha F_1 + (1-\alpha)F_2) = 0$. Since F_1 and F_2 are known, this leads to a cubic equation in α. There will be 1 or 3 real solutions (7 points and 2 camera centers form a quadric, if it is a ruled quadric, there will be 3 real solutions), and substituting it back in Equation 2 will give us the solution for the fundamental matrix. In the case of 3 real solutions, we performed RANSAC on all the candidate fundamental matrices and selected the one with the highest number of inliers obtained. We calculated fundamental matrices for each image pair to estimate inlier feature pairs. These inliers were then used as inputs to all the algorithms discussed below. Please note that we took inputs from online resources to implement our data loader.

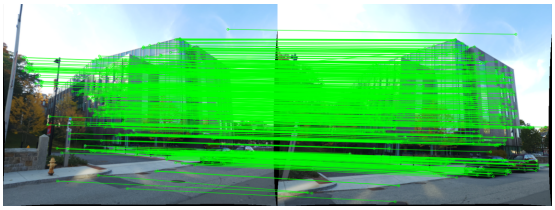

(a) Inliers

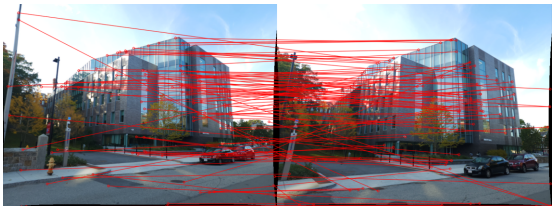

(b) Outliers

Fig. 1: RANSAC was used to detect inliers and outliers subjected to epipolar constraints for a given set of matched features.

B. Estimation of the essential matrix

Since the camera calibration matrix, K, was given, the essential matrix, E, can be calculated using Equation 4. The essential matrix was calculated using singular value decomposition (SVD) followed by rank reduction.

$$E = K^T F K \tag{3}$$

$$E = UDV^T \tag{4}$$

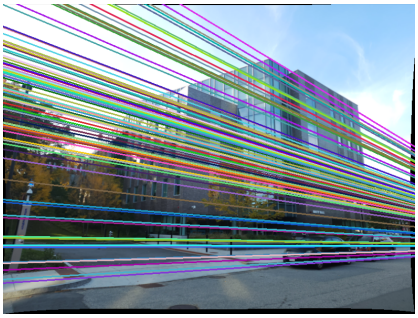

Fig. 2: Epilines for the first image features plotted on the second image.

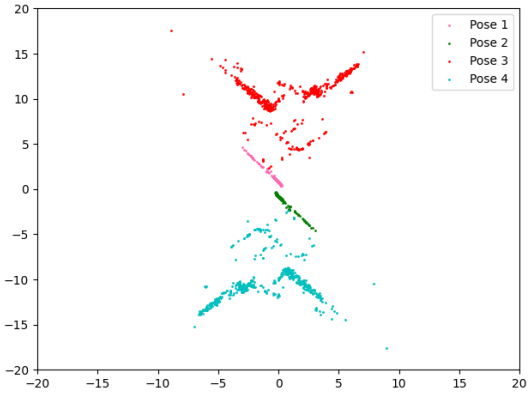

Fig. 3: Triangulated world points for all camera poses obtained after SVD of E.

C. Camera pose estimation from the essential matrix

After calculating the essential matrix, there will be 4 possible solutions for the camera pose (2 solutions for R and C).

$$C = \pm U_3 \tag{5}$$

$$R = U \begin{bmatrix} 0 & \pm 1 & 0 \\ \mp 1 & 0 & 0 \\ 0 & 0 & 1 \end{bmatrix} \tag{6}$$

$$\tag{7}$$

where U_3 is the third column of U. It is important to ensure that $R \in SO(3)$. Hence, if $det(R) < 0$, then $R = -R$ and $C = -C$.

D. Linear and non-linear triangulation subjected to cheriality constraints

Since there are 4 camera poses, the next step is to linearly triangulate all the feature points and evaluate the cheriality constraint which states that the world points must be in front of the image plane for both camera poses (depth > 0). Figure 3 shows a 2D plot (Y=0) of the triangulated points using all the candidate camera poses. To rule out three camera poses, we selected the camera pose that had the most number of features satisfying Equation 8.

Fig. 4: Improvement after non-linear triangulation

Fig. 5: Improvement in feature projection after non-linear PnP

$$r_3^T (X - C) > 0 \tag{8}$$

where r_3 is the third column of the candidate rotation matrix, C is the candidate translation vector and the world point X was calculated using linear triangulation. Since linear triangulation has no geometric meaning, we used non-linear optimization to minimize the reprojection error which improved the world point estimates. Figure 4 shows the refinement in feature locations after non-linear optimization.

E. Adding n^{th} image using perspective-n-point

To estimate n^{th} camera pose, we found feature points present in the first two images and the n^{th} image, and the corresponding world points obtained after non-linear triangulation. Since the intrinsic parameters, K, are known, we solved the following system of equations using SVD to obtain R and C.

$$\lambda x = K \begin{bmatrix} R & C \end{bmatrix} X \tag{9}$$

where x are the feature points, X are the corresponding world points and λ is the scaling factor. The value of R was corrected to ensure that it was a valid rotation matrix. This linear estimate acted as an initial guess for the non-linear optimization framework using reprojection error. Figure

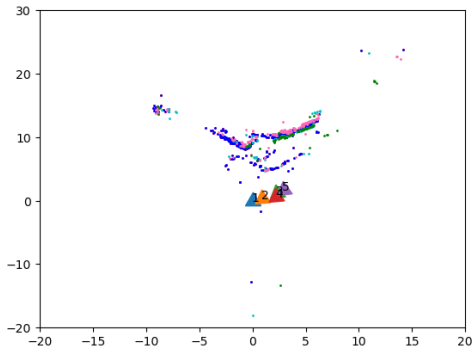

Fig. 6: Point cloud obtained after estimating world points using the first two images and registering all the other images using PnP.

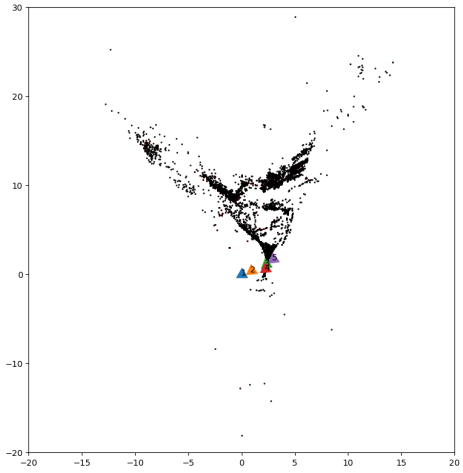

Fig. 7: Point Cloud including all the points from the matches file using PnP poses.

5 shows the improvement in feature projection after non-linear optimization. We perform this registration step for all the 3 images. The resulting point cloud and the estimated camera poses are illustrated in Figure 6.

	Mean Reprojection Error
Linear Triangulation	87.402
Non-Linear Triangulation	66.731
Linear Perspective-n-Point	88.609
Non-Linear Perspective-n-Point	9.997

TABLE I: We report the reprojection error averaged over all the images.

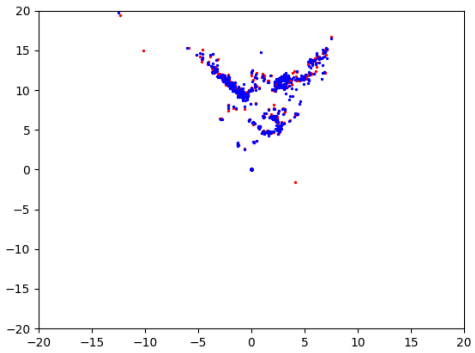

Fig. 8: Point cloud correction before and after bundle Adjustment. Red indicates before bundle adjustment and blue indicates after bundle adjustment for the 1st matching file.

F. Global optimization using bundle adjustment.

Bundle Adjustment was performed to optimize both the triangulated world points and camera poses. To facilitate this, we constructed a visibility matrix and generated a sparse matrix for **scipy.optimize.least_squares**. The results of point cloud triangulation using the first matching file were presented, revealing limited optimization potential due to the small number of points. However, a notable total shift of 23.30 in the L2 norm between the points was observed before and after bundle adjustment. This is illustrated by Figure 8.

REFERENCES

[1] R. Hartley and A. Zisserman, *Multiple View Geometry in Computer Vision*, 2nd ed. New York, NY, USA: Cambridge University Press, 2003.